CHEMICAL ENGINEERING TRANSACTIONS
VOL. 99, 2023
A publication of AIDIC
The Italian Association of Chemical Engineering
Online at www.cetjournal.it
Guest Editors: Sauro Pierucci, Flavio Manenti

**ISBN** 978-88-95608-98-3; **ISSN** 2283-9216
DOI: 10.3303/CET2399116

# Process Analysis of Integrated Biomass Gasification and Solid Oxide Electrolysis Cell (SOEC) for Syngas Production

Thanaphorn Detchusananard[a], Kunlanan Wiranarongkorn[b], Karittha Im-orb[c,*]

[a] Center of Excellence in Process and Energy Systems Engineering, Department of Chemical Engineering, Faculty of Engineering, Chulalongkorn University, Bangkok 10330, Thailand
[b] Department of Basic Science and Physical Education, Faculty of Science at Sriracha, Kasetsart University Sriracha Campus, Chonburi 20230, Thailand
[c] Program in Food Process Engineering, School of Food-Industry, King Mongkut's Institute of Technology Ladkrabang, Bangkok 10520, Thailand
karittha.im@kmitl.ac.th

The integrated biomass gasification and SOEC process (IBG-SOEC), which $O_2$ from SOEC was used as gasifying agent while the separated $H_2$ could be used for $H_2$/CO adjustment or sell as a valuable byproduct, was studied to find the sustainable syngas production process. The model of IBG-SOEC was developed in Aspen Plus. The parametric analysis was performed to investigate the effect of operating conditions of SOEC (i.e., cell temperature and number of cells) on the overall process performance. For energy performance, the total energy demand decreased as cell temperature increased while increased with number of cells. The changes in cell temperature had no effect on the yield and composition of syngas from gasifier. The maximum yield of syngas, with $H_2$/CO of 0.96, of 1.9 kmol/h was achieved at cell temperature of 790 °C and number of cells of 600. At this condition, the overall efficiency of IBG-SOEC of 63 % was achieved and $H_2$ byproduct of 1 kmol/h could obtained from SOEC.

## 1. Introduction

Biomass gasification is a promising technology for converting biomass into syngas (mainly contain $H_2$ and CO) which can be direct used as a fuel gas or as an intermediate for several chemical synthesis. In the process, biomass reacts with gasifying agent, which can be air, steam, $O_2$, $CO_2$ or the mixture of them, to produce syngas. The use of different gasifying agents provides syngas with different $H_2$/CO ratios. Islam (2020) reported that using steam as gasifying agent offered the syngas with the highest $H_2$/CO ratio followed by using $H_2O_2$, air, $O_2$ and $CO_2$, respectively. Commercially, although the use of air and $O_2$ as gasifying agent were preferred due to the high energy demand of steam generation, it provides low $H_2$/CO syngas. Therefore, the water gas shift (WGS) and the carbon capture and utilization system (CCUS) units were needed to increase $H_2$ and decrease $CO_2$, respectively. However, this practice offered lower carbon conversion efficiency of the total system (Sun and Tang, 2023). In addition, direct feeding $H_2$ to the syngas can be another option. However, $H_2$ was mainly produced from fossil fuel via steam reforming of natural gas or coal gasification which causes an increase in atmospheric $CO_2$ level. The water electrolysis is an interesting technology for green $H_2$ production as it uses renewable electric energy to separate water into $H_2$ and $O_2$. There are several types of water electrolyzer including alkaline electrolyte membrane (AEL), polymer electrolyte membrane (PEM) and solid oxide electrolysis cell (SOEC). As the SOEC operated at high temperature (600-800 °C) closed to gasifying temperature (Im-orb et al., 2018), the integration of biomass gasification and SOEC could provide the more energy efficient and sustainable syngas production process. In addition, this integrated system could consequently integrate with some chemical synthesis. For example, Giglio et al. (2021) studied the integration of biomass gasification, SOEC and methane synthesis. They found that the process without additional WGS and CCUS offered high overall process efficiency of 71.7 %. Clausen et al. (2019) reported that 70 % of energy efficiency was achieved when using the integration of steam electrolysis and biomass gasification for synthetic natural gas (SNG) production.

Paper Received: 28 February 2023; Revised: 14 March 2023; Accepted: 6 May 2023
Please cite this article as: Detchusananard T., Wiranarongkorn K., Im-Orb K., 2023, Process Analysis of Integrated Biomass Gasification and Solid Oxide Electrolysis Cell (SOEC) for Syngas Production, Chemical Engineering Transactions, 99, 691-696 DOI:10.3303/CET2399116

Ali et al. (2020) studied an integration of oxygen blown biomass gasification, SOEC and methanol synthesis. In their result, the thermal efficiency of 72.08 % was obtained by using oxygen generated form SOEC as gasifying agent. Previously, most studies focused on the process analysis of the overall process of biochemicals (e.g., methane, methanol and DME) production in several aspects. Nevertheless, the intensive study on the syngas production part via the integrated biomass gasification and SOEC still lack of study. Therefore, the objective of this study is to perform the process analysis of the integrated biomass gasification and SOEC process (IBG-SOEC) for syngas production. The effect of cell temperature of SOEC and number of cells on the overall IBG-SOEC performance was investigated. The simplify process of IBG-SOEC was shown in Figure 1.

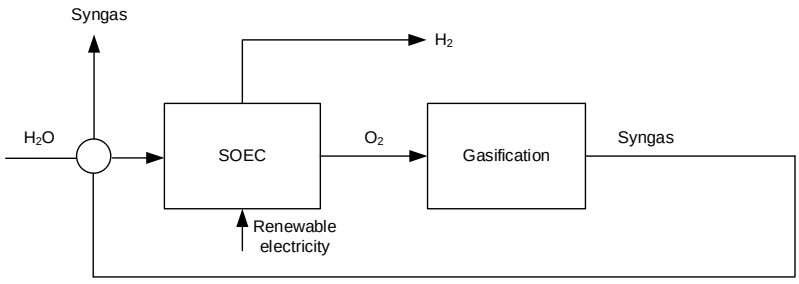


*Figure 1: Simplify diagram of the IBG-SOEC.*

## 2. Model development

In this study, the renewable electricity was supplied to SOEC to separate $H_2O$ into $O_2$ and $H_2$. Then $O_2$ was fed to gasifier as gasifying agent and reacted with biomass to produce syngas. The $H_2$ derived from SOEC was separated as valuable byproduct. The model of the IBG-SOEC, developed in Aspen Plus software version 10, consisted of two-main parts, i.e., biomass gasification and SOEC (Figure 2). The empty fruit branch (EFB) of oil palm was used as biomass feedstock and its proximate and ultimate analyses was shown in Table 1.

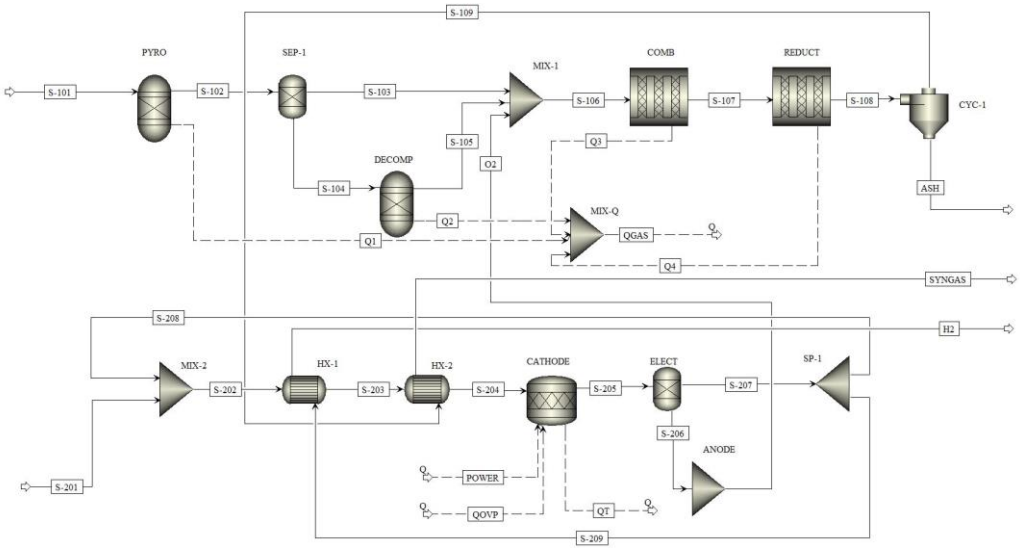


*Figure 2: Aspen plus model flowsheet of the IBG-SOEC.*

*Table 1: Ultimate and proximate analyses of EFB (Uthaikiattikul et al., 2011)*

| Ultimate Analysis | (wt.% dry biomass) | Proximate Analysis | (wt.% dry biomass) |
|---|---|---|---|
| Carbon | 43.78 | Fixed carbon | 13.31 |
| Hydrogen | 6.2 | Volatile matter | 79.82 |
| Oxygen | 42.62 | Ash | 6.87 |
| Nitrogen | 0.44 | Moisture | 12.5 |
| Sulfur | 0.09 | | |

### 2.1 Biomass gasification

As shown in Figure 2, the model of biomass gasification comprised of four major sections, i.e., pyrolysis, decomposition, combustion, and reduction. Biomass (S-101) was fed to the pyrolysis section (PYRO), modeled by RYIEL to produce the pyrolysis product containing of $H_2$, CO, $CO_2$, $CH_4$ $C_2H_4$, $C_2H_6$, $C_6H_6$, $C_7H_8$, $C_6H_6O$, $C_{10}H_8$ and $H_2O$ (Eq(1)). The yields of pyrolysis product were calculated from the correlations of yield of pyrolyzed products and pyrolysis temperature, and the yield of biochar was derived from mass balance (Abdelouahed et al., 2012). Then non-conventional biochar was separated at a separator (SEP) before it was converted to conventional components, including C, $O_2$, $N_2$, $H_2$, S and ash at decomposition section (DECOM), modelled by RYIELD, in which the yield distribution based on ultimate and proximate analyses was specified. The pyrolysis gases (S-103) and biochar (S-105) reacted with $O_2$ from the SOEC at the combustion section (COMB), modelled by RPlug, in which the oxidation reactions occurred (Eq(2)-Eq(7)). Then, the product gases from this section were sent to the reduction section (REDUCT), modelled by RPlug, in which the reduction reactions occurred (Eq(8)-Eq(14)). The composition of syngas from the combustion and reduction sections was determined based on the kinetic data of related oxidation and reduction reactions (Puig-Gamero et al., 2021). The reactions considered in gasification section were summarized in Table 2. In this study, the developed gasification model was validated with the experimental data reported by Pio et al. (2017) and offered comparable results with the root mean square error of 1.09%.

*Table 2: The related reactions in gasification process*

| Reactions | | |
|---|---|---|
| **Pyrolysis section** | | |
| Biomass pyrolysis | $Biomass \rightarrow CH_4 + H_2 + CO + C_2H_4 + C_2H_6 + C_6H_6 + C_7H_8 + C_6H_6O_6 + C_{10}H_8 + H_2O + biochar$ | (1) |
| **Combustion section** | | |
| Partial oxidation of C | $\alpha C(s) + O_2 \rightarrow 2(\alpha - 1)CO + (2 - \alpha)CO_2$ | (2) |
| Partial oxidation of $CH_4$ | $CH_4 + 1/2O_2 \rightarrow CO + 2H_2$ | (3) |
| Total oxidation of CO | $CO + 1/2O_2 \rightarrow CO_2$ | (4) |
| Hydrogen oxidation | $H_2 + 1/2O_2 \rightarrow H_2O$ | (5) |
| Partial oxidation of benzene | $C_6H_6 + 9/2O_2 \rightarrow 6CO + 3H_2O$ | (6) |
| Partial oxidation of phenol | $C_6H_6O + 4O_2 \rightarrow 6CO + 3H_2O$ | (7) |
| **Reduction section** | | |
| Water gas shift | $CO + H_2O \rightarrow CO_2 + H_2$ | (8) |
| Water gas | $C + H_2O \rightarrow CO + H_2$ | (9) |
| Boudouard | $C + CO_2 \rightarrow 2CO$ | (10) |
| Steam reforming | $CH_4 + H_2O \rightarrow CO + 3H_2$ | (11) |
| Decomposition of phenol | $C_6H_6O \rightarrow CO + 0.4C_{10}H_8 + 0.15C_6H_6 + 0.1CH_4 + 0.75H_2$ | (12) |
| Decomposition of naphthalene | $C_{10}H_8 \rightarrow 6.5C + 0.5C_6H_6 + 0.5CH_4 + 1.5H_2$ | (13) |
| Steam reforming of phenol | $C_6H_6O + 3H_2O \rightarrow 4CO + 0.5C_2H_4 + CH_4 + 3H_2$ | (14) |

### 2.2 Solid oxide electrolysis cell

The SOEC consisted of an electrolyte, a cathode and an anode, which were normally constructed from yttria-stabilized zirconia cermet (YSZ), Ni-yttria-stabilized zirconia cermet (Ni-YSZ) and lanthanum strontium manganite-YSZ (LSM-YSZ), respectively. The model of SOEC was developed based on the same approach as reported in previous work (Im-orb et al., 2018). The RSTOIC reactor represented the cathode (CATHODE), in which the electrochemical reaction of the steam was occurred at specified reaction temperature to produce $H_2$ and $O_2$. Then, $O_2$ was separated from $H_2$ through an electrolyte (ELECT), which was modelled by SEPARATOR, and completely permeated into the anode channel (ANODE). The electrolysis reactions occurred in SOEC were shown in Table 3. The equations used to calculate the SOEC performance and the overall efficiency of the process were summarized in Table 4. As shown in Eq(17), the cell voltage of SOEC calculated by the summation of the equilibrium voltage and all overpotential, i.e., ohmic overpotential (Eq(20)), activation overpotential (Eq(21)-Eq(23)), and concentration overpotential (Eq(24)-Eq(26)). The total electricity requirement for the SOEC can be computed by multiplying of the current density (*J*), cell voltage (*V*), cell area (*A*), and number of cells (*N*) in the SOEC stack as shown in Eq(27). For the IBG-SOEC performance, the overall efficiency could be evaluated by the lower heating value (LHV) of the products (e.g. syngas and $H_2$) divided by total energy input (Eq(30)).

*Table 3: The electrolysis reactions in SOEC*

| | Reactions | |
|---|---|---|
| Cathode | $H_2O + 2e^- \rightarrow H_2 + O^{2-}$ | (15) |
| Anode | $O^{2-} \rightarrow \frac{1}{2}O_2 + 2e^-$ | (16) |

*Table 4: The equations for calculation of SOEC and overall IBG-SOEC performance*

| | Equations | |
|---|---|---|
| Cell voltage ($V$) | $V = E + \left(\eta_{\text{ohmic}} + \eta_{\text{act}} + \eta_{\text{conc}}\right)$ | (17) |
| Equilibrium voltage ($E$) | $E = E^0 + \frac{RT}{2F}\ln\left(\frac{x_{H_2} \cdot x_{O_2}^{1/2} \cdot P^{1/2}}{x_{H_2O}}\right)$ | (18) |
| Standard potential ($E^0$) | $E^0 = 1.253 - 2.4516\times10^{-4}T$ | (19) |
| Ohmic overpotential ($\eta_{\text{ohmic}}$) | $\eta_{ohm} = 2.99\times10^{-5} JL \exp\left(\frac{10300}{T}\right)$ | (20) |
| Activation overpotential ($\eta_{\text{act}}$) | $\eta_{act} = \eta_{act,a} + \eta_{act,c}$ | (21) |
| | $\eta_{act,i} = \frac{RT}{F}\ln\left[\frac{J}{2J_{0,i}} + \sqrt{\left(\frac{J}{2J_{0,i}}\right)^2 + 1}\right]$, $i$ = a or c | (22) |
| | $J_{0,i} = \gamma_i \exp\left(-\frac{E_{act,i}}{RT}\right)$, $i$ = a or c | (23) |
| Concentration overpotential ($\eta_{\text{conc}}$) | $\eta_{conc} = \eta_{conc,a} + \eta_{conc,c}$ | (24) |
| | $\eta_{conc,a} = \frac{RT}{4F}\ln\left(\frac{\sqrt{\left(P_{O_2}^0\right)^2 + \left(JRT\mu d_a / 2FB_g\right)}}{P_{O_2}^0}\right)$ | (25) |
| | $\eta_{conc,c} = \frac{RT}{2F}\ln\left[\frac{\left(P_{H_2} + JRTd_c / 2FD_{H_2O}^{eff}\right)\cdot P_{H_2O}}{\left(P_{H_2O} - JRTd_c / 2FD_{H_2O}^{eff}\right)\cdot P_{H_2}}\right]$ | (26) |
| Power ($W$) | $W = J \cdot V \cdot A \cdot N$ | (27) |
| Thermal energy for SOEC ($Q_{\text{T,SOEC}}$) | $Q_{\text{T,SOEC}} = Q_{\text{r}} - Q_{\text{ovg}} - W$ | (28) |
| Heat of overpotential ($Q_{\text{ovg}}$) | $Q_{\text{ovg}} = \left(\eta_{\text{ohmic}} + \eta_{\text{act}} + \eta_{\text{conc}}\right)\cdot J \cdot A \cdot N$ | (29) |
| Overall efficiency ($\eta_{\text{en}}$) | $\eta_{\text{en}} = \frac{\dot{N}_{\text{SYGN}} LHV_{\text{SYGN}} + \dot{N}_{\text{H}_2} LHV_{\text{H}_2}}{W + Q_{\text{T,SOEC}} + Q_{\text{T,GAS}} + \dot{M}_{\text{EFB}} LHV_{\text{EFB}}} \cdot 100$ | (30) |

## 3. Results and discussions

### 3.1 Effect of cell temperature of SOEC on overall IBG-SOEC performance

In this section, the effect of cell temperature of SOEC on the IBG-SOEC performance was investigated by varying the cell temperature in a range of 700-850 °C at constant number of cells of 400. Figure 3a showed that the activation overpotential and ohmic overpotential decreased whereas the concentration overpotential increased as the cell temperature increased. This was due to an increase in the rate of electrochemical reaction and oxygen ion conductivity of electrolyte at elevated cell temperature. Moreover, the equilibrium voltage decreased when cell temperature increased resulting in lower cell voltage. This led to lower electrical demand as shown in Figure 3b. Although thermal energy demand increased, the total energy demand slightly decreased. The overall efficiency of IBG-SOEC was found to increase as cell temperature increased from 700 to 790 °C and reached the maximum value of 63 % before it started to decrease when the cell temperature higher than this range. At the cell temperature higher than 790 °C, the overall efficiency decreased due to the increase in

thermal energy demand. It was noted that the cell temperature had no effect on the yield and composition of syngas produced from gasifier.

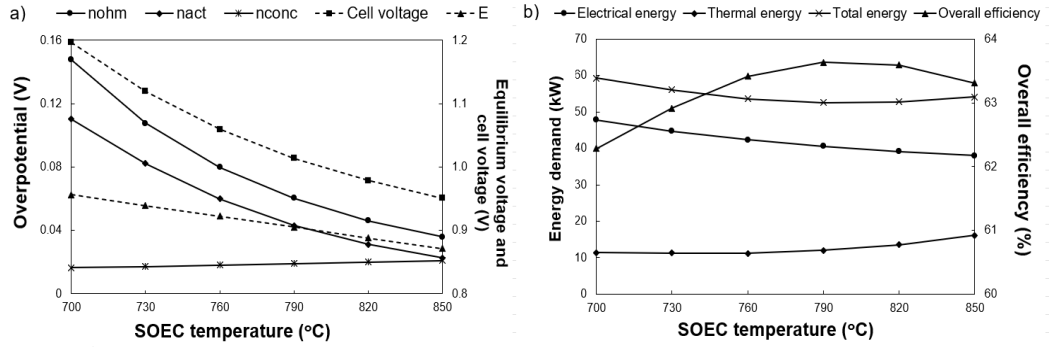


*Figure 3: Effect of cell temperature on a) overpotential, equilibrium voltage and cell voltage, and b) energy demand and overall efficiency*

### 3.2 Effect of number of cells of SOEC on overall IBG-SOEC process performance

The effect of number of cells of SOEC on the IBG-SOEC performance was studied by varying the number of cells between 400-600 cells at constant temperature of 790 °C. Figure 4a indicated that increase in number of cells enhanced $O_2$ produced from SOEC leading to more gasifying agent fed to the gasifier. As a result, the amount of CO, $CO_2$ and $H_2$ produced from gasifier increased whereas $CH_4$ decreased due to the domination of oxidation reactions (Eq(2)-Eq(7)). Consequently, this increased the yield ($H_2$+CO) and the $H_2$/CO ratio of syngas as shown in Figure 4b. Moreover, $H_2$ from the SOEC, which could be sold as high value product or used to adjust the $H_2$/CO ratio of syngas to satisfy each chemical synthesis specification, was found to increase. The maximum yield of syngas of 1.9 kmol/h was achieved at number of cells of 600. At this condition, the $H_2$/CO ratio of 0.96 was obtained. Regarding the energy performance of the proposed process, the electricity demand increased while thermal energy demand decreased when number of cells increased resulting in an increase in the total energy demand. However, the overall efficiency was found to increase with number of cells caused by the reduction in thermal energy requirement (Figure 4c).

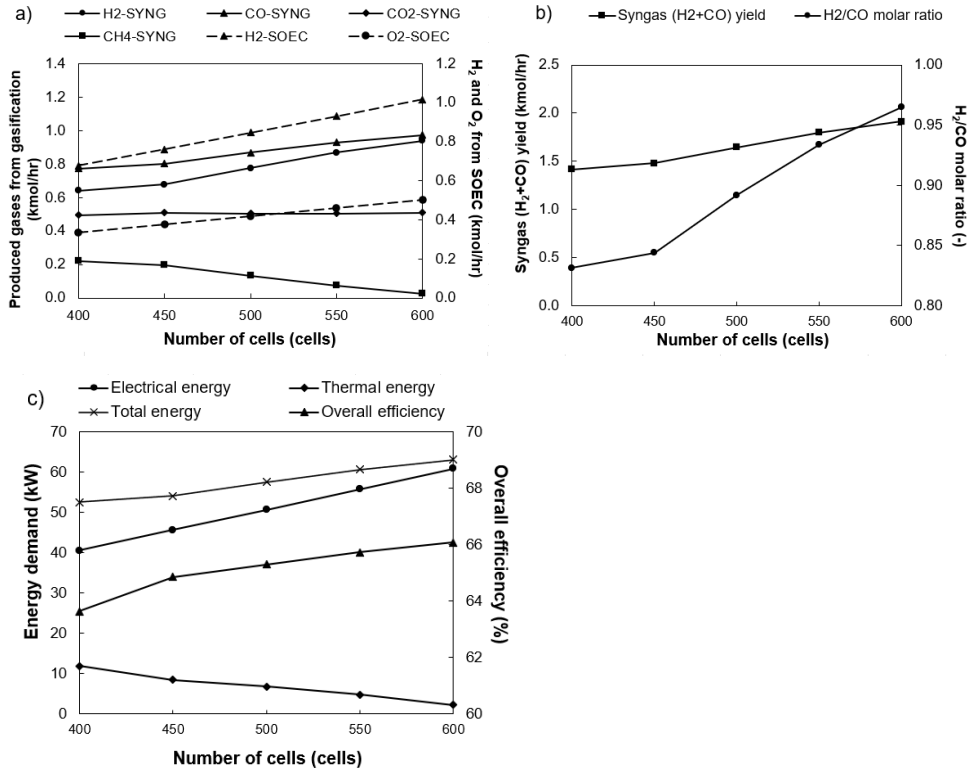


*Figure 4: Effect of number of cells on a) syngas composition and $H_2$ and $O_2$ from SOEC, b) syngas yield and $H_2$/CO ratio, and c) energy demand and overall efficiency*

## 4. Conclusions

The effect of operating conditions of SOEC i.e., cell temperature and number of cells, on the overall performance of the IBG-SOEC integrated process was investigated using process model developed in Aspen Plus. The overall energy demand was found to decrease when cell temperature increased whereas it increased with number of cells. The maximum efficiency of the IBG-SOEC of 63 % was achieved at cell temperature of 790 °C. Regarding the syngas production, the cell temperature had no effect on the yield ($H_2$+CO) and the $H_2$/CO ratio of syngas while the increase in number of cells could increase the yield and $H_2$/CO ratio of syngas. When the SOEC was operated at the cell temperature of 790 °C and the number of cells was maintained at 600, the maximum yield of syngas of 1.9 kmol/h obtaining $H_2$/CO ratio of 0.96 was achieved.

### Nomenclature

$A$ – cell area, $m^2$
$B_g$ – flow permeability, $m^2$
$D_{H_2O}^{eff}$ – effective diffusion coefficient of steam, $m^2/s$
$d_a$ – thickness of the anode, m
$d_c$ – thickness of the cathode, m
$E$ – equilibrium voltage, V
$E^0$ – standard potential, V
$E_{act}$ – activation energy, J/(mol·K)
$F$ – Faraday's constant, C/mol
$J$ – current density, $A/m^2$
$J_0$ – exchange current density, $A/m^2$
$L$– thickness of the electrolyte, m
$N$ – number of cells, cells
$\dot{M}$ – mass flow rate, kg/hr
$\dot{N}$ – molar flow rate, kmol/hr
$P$ – operating pressure, atm
$P_i$ – partial pressure of component i, Pa
$Q_r$ – heat required for the reaction, kW
$Q_{T,GAS}$ – thermal energy for gasification, kW
$Q_{T,SOEC}$ – thermal energy for SOEC, kW
$Q_{ovg}$ – heat of overpotential, kW
$T$ – cell temperature, K
$V$ – cell voltage, V
$W$ – power, V
x – mole fraction, -
$\eta_{act}$ – activation overpotential, V
$\eta_{conc}$ – concentration overpotential, V
$\eta_{en}$ – overall efficiency, %
$\eta_{ohmic}$ – ohmic overpotential, V

### Acknowledgments

This work was supported by King Mongkut's institute of Technology Ladkrabang (KREF046606).

### References

Abdelouahed L., Authier O., Mauviel G., Corriou J. P., Verdier G., Dufour A., 2012, Detailed Modeling of Biomass Gasification in Dual Fluidized Bed Reactors under Aspen Plus, Energy Fuels, 26, 3840-3855.

Ali S., Sorensen K., Nielsen M.P., 2020, Modelling a novel combined solid oxide electrolysis cell (SOEC)-Biomass gasification renewable methanol production system, Renewable Energy, 154, 1025-1034.

Clausen L.R., Butera G., Jensen S.H., 2019, High efficiency SNG production from biomass and electricity by integrating gasification with pressurized solid oxide electrolysis cells, Energy, 172, 1117-1131.

Giglio E., Vitalel G., Lanzini A., Santarelli M., 2021, Integration between biomass gasification and high temperature electrolysis cells for synthetic methane production, Biomass Bioenergy, 148, 106017.

Im-orb K., Visitdumrongkul N., Seabea D., Patcharavorachot Y., Arpornwichanop A., 2018, Flowsheet-based model and exergy analysis of solid oxide electrolysis cells for clean hydrogen production, Journal of Cleaner Production, 170, 1–13.

Islam M. W., 2020, Effect of different gasifying agents (steam, $H_2O_2$, oxygen, $CO_2$, and air) on gasification parameters, International Journal of Hydrogen Energy, 45, 31760–31774.

Pio D.T., Tarelho L.A.C., Matos M.A.A., 2017, Characteristics of the gas produced during biomass direct gasification in an autothermal pilot-scale bubbling fluidized bed reactor, Energy, 120, 915-928.

Puig-Gamero M., Pio D.T., Tarelho L.A.C., Sánchez P., Sanchez-Silva L., 2021, Simulation of biomass gasification in bubbling fluidized bed reactor using aspen plus, Energy Conversion and Management, 235, 113981.

Sun Y., Tang Y., 2023, Municipal solid waste gasification integrated with water electrolysis technology for fuel production: A comparative analysis, Chemical Engineering Research and Design, 191, 14–26.

Uthaikiattikul T., Kerdsuwan S., Laohalidanond K., Cherdphong S., 2011, Improvement of Producer Gas of Palm Oil Empty Fruit Bunch in a 50 kg/hr Prototype Downdraft Gasifier by Palletization, 4th International Conference on Sustainable Energy and Environment (SEE 2011): A Paradigm Shift to Low Carbon Society. 27-29 February 2012, Bangkok, Thailand